Transactions of the Materials Research Society of Japan 29 [8] 3415-3418 (2004)

Titanium Dioxide Nano-Particles through Thermal Plasma Oxidation of Titanium Nitride Powders

Takamasa Ishigaki*, Seung-Min Oh* and Dong-Wha Park**
*National Institute for Materials Science, Advanced Materials Laboratory,
1-1 Namiki, Tsukuba-shi, Ibaraki 305-0044, Japan
**Inha University, Department of Chemical Engineering,
Nam-gu, Incheon 402-751, Korea
Fax: 81-29-860-4701, e-mail: ISHIGAKI.Takamasa@nims.go.jp

Titanium dioxide nano-particles were synthesized by in-flight oxidation of micron-scale titanium nitride powders using inductive thermal plasma. The reaction was carried out initially by surface oxidation of titanium nitride, leading to core-shell composites with oxidized shells and titanium nitride cores, followed by the gas phase synthesis of nano-sized titanium dioxide from vaporized species. At deficient oxygen content, the black colored shell was mainly made up of rutile and nano-sized powders solidified from vapor species co-existing with anatase and rutile. With an increasing oxygen flow rate, the micron sized composites were rapidly oxidized, simultaneously enhancing vaporization and size reduction. Spherical anatase crystals were obtained under excessive oxygen input conditions.
Key words: thermal plasma, titanium oxide, anatase crystal, nanopowder.

1. INTRODUCTION

Titanium dioxide has recently been a subject of interest as a photocatalyst, photonic crystal, photovoltaic cell, nanoceramics, or sensors. The key properties to improve the efficiencies in applications are related to structure, phase composition, size, and morphology. Titanium dioxide is known to have three polymorphic forms: thermodynamic stable rutile, metastable anatase, and brookite found only as a natural single crystal. Anatase phase easily transforms to rutile over a wide range of temperature, but the formation mechanism and effects of additives on the phase transformation are not fully understood. The industrial production of this material is known to mature technology through the chloride and sulfate process, and recent research on the preparation tends toward sol-gel process[1-3], flame synthesis[4-6], and thermal plasma synthesis[7-9]. The main disadvantages of sol-gel involve a large quantity of organic solvents and particle growth caused by further heat treatment. Flame synthesis is relatively inexpensive and simple, but the phase control for pure titanium dioxide is difficult because of high temperature and limited input gases. Vemury and Pratsinis have been investigating the effect of dopants on flame synthesis to control the phase composition and the size of titanium dioxide[5].

Thermal plasma synthesis is known to be a clean process with less off gases and a one-step high throughput process because of the extremely high temperature and high reaction rate[10]. The distinct advantage of this process is that it does not introduce foreign impurities, and recently a wide range of nanopowders were prepared by using this process [11-13].

In this paper, we focus on the preparation of titanium dioxide from titanium nitride using Ar-O_2 thermal plasma. The process parameter relating to phase composition, crystal size, and morphology is also discussed. It is clear that the formation of anatase and rutile is influenced mainly by oxygen input conditions in thermal plasma process.

2. EXPERIMENTS

The RF thermal plasma torch and reactor chamber used in the present study have been reported elsewhere [16,17]. The water-cooled plasma torch(Model PL-50, TENKA Plasma System Inc., Canada) was connected to a 2 MHz radio frequency power supply(Nihon Koshuha Co. Ltd., Japan) and attached to a water-cooled cylindrical reactor. For introduction of raw material, a water-cooled probe was injected into the center of the plasma torch along the axis.

The starting powder of titanium nitride with diameter of ave. 28 ㎛ (Nippon New Metals Co., Japan) was injected into plasma plum through the water-cooled probe by a powder feeder using carrier gas, and the feed rate of powder was controlled to be about 1.5 g/min by adjusting the motor speed of the feeder. The sheath gas, which protects the inner wall of the tube from extremely high temperature, is properly mixed with the central plasma stream only at a substantial distance from the torch exit plane. Ar+O_2 plasma were generated by mixing O_2 in Ar sheath gas. Pure Ar was used as the powder carrier gas. The flow rate of O_2 was varied up to 40 l/min, and the total flow rate of central, sheath, and carrier gas was typically 30 l/min, 90 l/min, and 5 l/min, respectively. The plasma was discharged with the plate power of 25 kW.

3. RESULTS AND DISCUSSION

The TiN powders were rapidly oxidized and partially vaporized in substantial residence time in high velocity plasma stream. Fig. 1 shows the X-ray diffraction patterns of the powders synthesized at a different O_2 flow mixed in Ar sheath gas, and the products were collected mainly at the reactor wall. As the O_2 flow rate was increased, the peaks corresponding to TiO_2 increased because of enhanced oxidation, and the

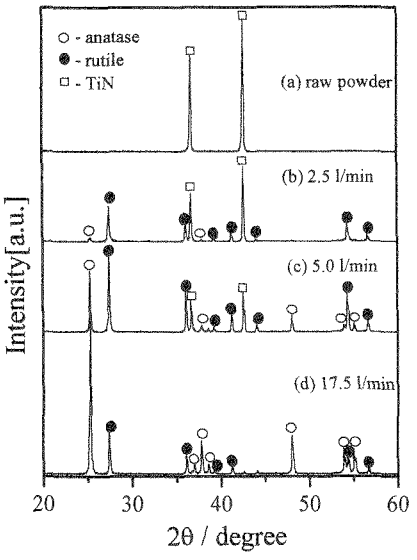

Fig. 1 X-ray diffraction patterns of the powders synthesized at different oxygen flow.

patterns of the powders synthesized at higher O_2 input exceeding 10 l/min showed only the lines corresponding to TiO_2 consisting of anatase[JCPDS 21-1272] and rutile[JCPDS 21-1276]. The product synthesized under the higher O_2 input conditions is composed mainly of anatase as shown in Fig. 1d.

As-produced powders typically consist of coarse-grain powders and fine-grain ones as shown in Fig. 2. The morphology of large grain powders implies the degree of oxidation for individual particles, which are related to different particle trajectories for in-flight oxidation in plasma plum. The oxidation reaction promotes the spherodization of coarse-grained raw powders and reduces the size by enhanced vaporization, because the melting and boiling point of oxidized surface are lower than that of raw powders. The hollow structures in Fig. 2c are attributed to rapid oxidation and melting that lead to the formation of oxide shell, which was followed by further evaporation from inside the particles by oxygen diffusion. Small grain powders separated from the surface of large grain powders revealed themselves to be uniform in size and nano-sized powders as shown in Fig. 2d.

The weight fraction of anatase and vapor fractions in product powders was plotted as a function of O_2 content in plasma stream as shown in Fig. 3. Under low O_2 input condition, anatase phase was not detected in large grain powders, and only a small amount of powders was vaporized because of improper oxidization of TiN. The anatase content of large grain powders and vapor fraction rapidly increased up to 80 wt% with the increasing oxygen O_2 content. The result implies that the phase composition is not influenced by the anatase to rutile transformation by heat treatment, because heat transfer is enhanced by added oxygen and exothermic reaction heat. The formation mechanism of anatase and rutile is elucidated as follows. The surface of the powders is rapidly oxidized and molten, leading to composite melts composed of TiO_2 shells and TiN cores. The composites are solidified to anatase or rutile

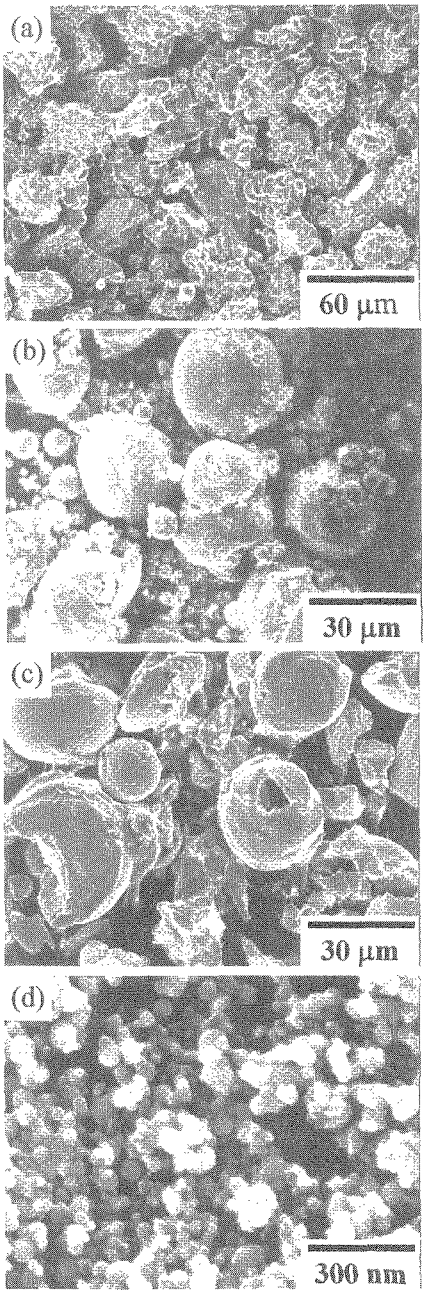

Fig. 2 Morphology of the powders synthesized from TiN by Ar-O_2 plasma: (a) raw powder; (b) as-produced powder synthesized at O_2 – 4 l/min; (c) large grain powders and (d) small grain powders separated from (b).

depending on the oxygen content. At low oxygen input, the composite melts could be easily formed of oxygen defect structure by diffusion of oxygen into the cores, and oxygen vacancy in TiO_2 structure cause the formation of rutile. With the increasing the oxygen input, the oxidation of powders is promoted thus the oxidized surface is impelled to vaporize because of exothermic reaction heat and lowered boiling point of the powder, leading to the rapid increase of vapor fraction. Under higher O_2 input condition, the composites become completely oxidized to TiO_2 melts, and rapid quenching

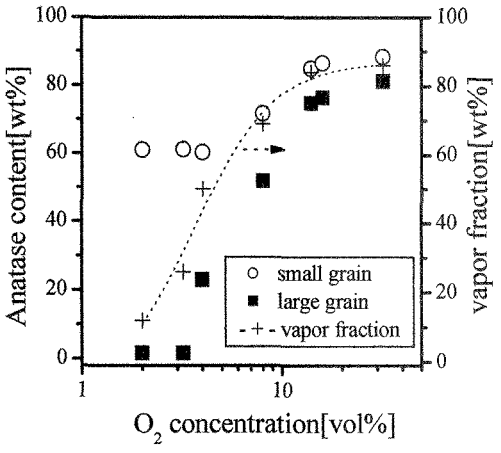

Fig. 3 Relative weight fractions of anatase and vapor fractions for the products as a function of O_2 concentration in plasma stream.

of the melts cause the anatase crystals. The formation of metastable anatase crystal from TiO_2 melt is consistent with the classical nucleation theory that critical free energy for nucleation of metastable phase is lower than that of the stable phase[14]. The anatase content did not significantly change at the concentration of O_2 < 5%, and it is probably related to the impelled vaporization of powders, because oxygen-deficient clusters would be easily transform to rutile clusters[15]. With the increasing of O_2 input, the anatase content increased up to 90%. The formation mechanism of anatase and rutile nanopowders is elucidated in terms of O_2 concentrations; the anatase is formed by solidification of the oxygen-rich gas mixture under higher O_2 concentrations, while the rutile is derived from the oxygen-deficient gas mixture.

Figure 4 shows the SEM images of the large grain powders and nanopowders separated from as-produced powders. The coarse powders in Fig. 4a are derived from partially melted surface by partial oxidation under low O_2 input condition. The large grain powders are significantly reduced in size with the increasing O_2 flow rate because of the enhanced vaporization, and spherodization of powders was induced from molten oxides. Under higher O_2 input conditions, the formation of spherical crystals, corresponding to anatase as shown in Fig. 3, is due to the rapid solidification of fully oxidized TiO_2 melt. In the case of gas phase synthesis, the size of the nanopowders increased from ave. 50 nm to 70 nm according to the O_2 flow rate and it is associated to the phase composition. The polyhedral shaped nanopowders in b is of the rutile phase, while spherical nanopowders in d is of the anatase grown from oxygen-rich clusters.

4. SUMMARY

We have prepared spherical single crystals of anatase and rutile nanopowders using Ar-O_2 thermal plasma. The results led us to conclude that the compositions of oxidized powders depended mainly on the oxygen input conditions. The formation mechanism of rutile and anatase by in-flight oxidation of TiN was suggested as

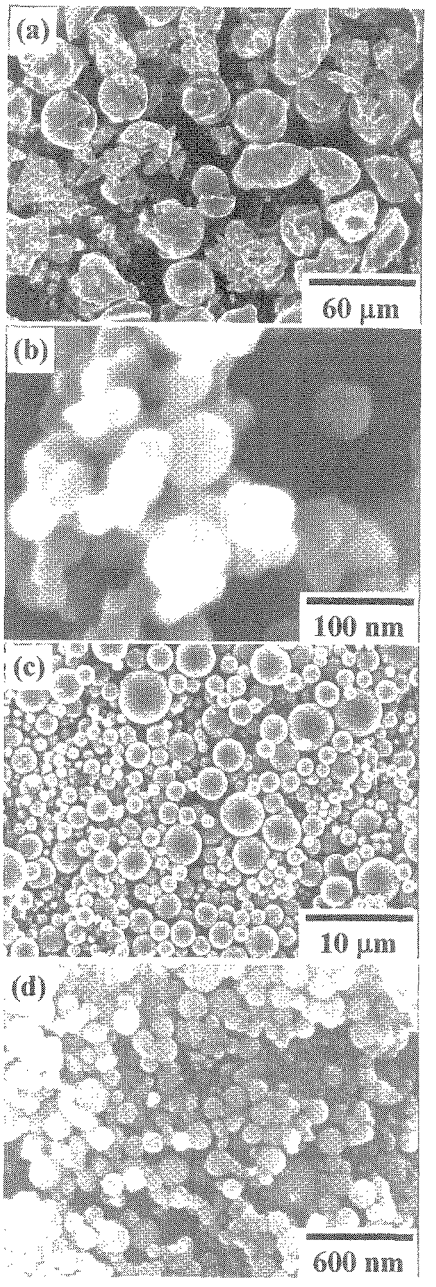

Fig. 4 SEM images of the large powders (a, c) and small powders (b, d): (a) and (b), O_2-2.5 l/min; (c) and (d), O_2-20 l/min.

follows. The surface of raw powders is initially oxidized to TiO sub-oxides and then rapidly formed to TiO_2 melts in the plasma stream, resulting in the formation of core-shell structured composites consisting of TiN cores and TiO_2 shells. Oxygen species is rapidly diffused from the TiO_2 melt into the cores and vaporization is impelled by lowered boiling point of oxidized surface. Under the low oxygen input conditions, the cores of the composites are not properly oxidized, thus they formed TiO sub-oxides or TiN, and the shell of TiO_2 melts was solidified to rutile phase because of the oxygen deficiency. The vaporized species from the oxidized

surface caused the formation of nanopowder, which coexists with anatase and rutile. With the increasing oxygen flow rate, the core-shell composites changed to fully oxidized TiO_2 melts and reduced in size by enhanced vaporization. The formation of spherical anatase single crystals is attributed to rapid solidification of fully oxidized TiO_2 melts under the high O_2 concentration.

REFERENCES

[1] J. Ovenstone, *J. Mater. Sci.*, **36**, 1325-1329(2001).
[2] C. C. Wang and J. Y. Ying, *Chem. Mater.*, **11**, 3113 -3120(1999).
[3] T. L. Hanley, V. Luca, I. Pickering and R. F. Howe, *J. Phys. Chem. B*, **106**, 1153-1160(2002).
[4] S. Vemury, S. E. Pratsinis and L. Kibbey, *J. Mater. Res.*, **12**, 1031-1042(1997).
[5] S. Vemury and S. E. Pratsinis, *J. Am. Ceram. Soc.*, **78**, 2984-2992(1995).
[6] H. D. Jang and S.-K. Kim, *Mater. Res. Bull.*, **36**, 627-637(2001).
[7] T. Ishigaki, Y.L. Li and E. Kataoka, *J. Am. Ceram. Soc.*, **86**, 1456-1463(2003).
[8] Y. L. Li and T. Ishigaki, *Chem. Mater.*, **13**, 1577 -1584(2001).
[9] S.-M. Oh, J.-G. Gong and D.-W. Park, *J. Chem. Eng. Jap.*, **34**, 283-287(2001).
[10] M. I. Boulos, P. Fauchais, and E. Pfender, Thermal Plasmas: Fundermentals and Applications, Vol. 1, Plenum Press, New York, 1994.
[11] O. Fukumasa, *Thin Solid Films*, **390**, 37-43(2001).
[12] P. V. Ananthapadmanabhan, P. R. Taylor, and W. Zhu, *J. Alloys and Compounds*, **287**, 126-129(1999).
[13] N. Rao, S. Girshick, J. Heberlein, P. McMurry, S. Jones, D. Hansen and B. Micheel, *Plasma Chem. Plasma Process.*, **15**, 581-603 (1995).
[14] Y.-L. Li, T. Ishigaki, *J. Crystal Growth*, **242**, 511 -516(2002).
[15] Y. Suyama, K. Ito, and A. Kato, *J. Inorg. Nucl. Chem.*, **37**, 1883-1888(1975).

(Received October 8, 2003; Accepted March 12, 2004)